

1 **Phase State and Physical Properties of Ambient and Laboratory**

2 **Generated Secondary Organic Aerosol**

3
4 **Rachel E. O'Brien,^{1,2*} Alexander Neu,¹ Scott A. Epstein,³ Amanda C. MacMillan,³**
5 **Bingbing Wang,⁴ Steve T. Kelly,¹ Sergey A. Nizkorodov,³ Alexander Laskin,⁴ Ryan C.**
6 **Moffet,² Mary K. Gilles,¹**

7 [1] Lawrence Berkeley National Laboratory, Berkeley, California, 94720-8198, USA

8 [2] Department of Chemistry, University of the Pacific, Stockton, CA 95211, USA

9 [3] Department of Chemistry, University of California, Irvine, CA 92697-2025, USA

10 [4] William R. Wiley Environmental and Molecular Sciences Laboratory, Pacific Northwest
11 National Laboratory, Richland, WA, 99352, USA

12
13 *Address correspondence to the following author

14 Email: resellon@lbl.gov

15
16
17
18
19
20
21
22
23

24 **Supplemental Information**

25

26 **Laboratory generated samples**

27 Experimental conditions for chamber experiments are given in Table S3 (the tables and
28 figures are numbered in the order of appearance in the main manuscript). For the flow tube
29 experiments, the flow tube was operated at low RH (< 2%), ambient temperature (~25 °C), with
30 the lights turned off. The oxidant was ozone (30-50 ppm) produced by flowing oxygen gas
31 through a commercial ozone generator. The residence time was ~5 min. In both cases (chamber
32 and flow tube) samples were collected on stages 7 and 8 of a 10 stage rotating cascade impactor
33 (MOUDI 110-R, MSP) using Si₃N₄ windows taped to aluminum substrates. Collection times
34 were ~30-45 min for chamber experiments and ~1 min for flow tube experiments.

35

36

37 **Data Collection/Analysis**

38 Because of the weak signal to noise ratio, particles with average OD₃₂₀ values < 0.03
39 were excluded from analysis. For I₀ values of ~ 7,000 counts/ms, this cutoff corresponds to
40 about 200 photons/ms. Since stray light in the STXM leads to approximately 100-200
41 photons/ms noise, the particles with the lowest average OD have the largest relative amount of
42 noise.

43 Since some particles and particle components were non-spherical, the sizes reported are
44 the area equivalent diameters (AED), defined as a diameter of a hemisphere required to cover the
45 same area as the projection of the particles on the surface:

46
$$\text{AED} = 2\sqrt{\left(\frac{\text{length}_x \times \text{length}_y}{\pi}\right)}$$
 Equation S1

47 where length_x and length_y are the effective sizes of the particle in the x and y dimensions.

48

49 **Absorption Coefficients**

50 Organic material mass absorption coefficients μ (cm^2/g) were obtained from the sum of
51 the absorption cross sections of the constituent atoms by:

52

53
$$\mu = \frac{N_A}{MW} \sum_i x_i \sigma_{ai}$$
 Equation S2

54

55 where MW is the molecular weight of the compound containing x_i atoms of type i , σ_a is the total
56 atomic absorption cross section (cm^2/atom) for this type of atom, and N_A is the Avogadro's
57 number. This approximation neglects interactions between the atoms in the material and is
58 applicable at photon energies sufficiently far from absorption edges [*Henke et al.*, 1993;
59 *Thomson et al.*, 2009]. Using the list of chemical formulas from negative mode high resolution
60 mass spectrometry analysis of ambient particles (O'Brien et al., manuscript in preparation,
61 2014), the mass absorption coefficient was calculated and plotted as a function of the O/C value
62 (Figure S3). An estimate for the average O/C value of 0.44 [*Setyan et al.*, 2012] leads to $\mu_{320} \cong$
63 $22,500 \text{ cm}^2/\text{g}$ and $\mu_{278} \cong 1102 \text{ cm}^2/\text{g}$.

64

65 **Inorganic Contributions**

66 The particles used in this analysis were identified as organic using algorithm detailed in
67 [*Moffet et al.*, 2010b]. However, aerosol particles that are primarily organic can also have

68 inorganic components. To estimate the fraction of other elements in these particles we examined
 69 the OD at the carbon pre-edge (278 eV) and the post edge (320 eV) of a particle with inorganic
 70 and organic components via equations S3 and S4:

71

$$72 \quad OD_{278} = \mu_{org,278}\rho_{org}d_{org} + \mu_{in,278}\rho_{in}d_{in} \quad \text{Equation S3}$$

$$73 \quad OD_{320} = \mu_{org,320}\rho_{org}d_{org} + \mu_{in,320}\rho_{in}d_{in} \quad \text{Equation S4}$$

74

75 Where μ_{org},ρ_{org} is the linear absorption coefficient of the organic species, μ_{in},ρ_{in} is the linear
 76 absorption coefficient for the inorganic species, and d_{in} and d_{org} are the average sample
 77 thicknesses of the inorganic and organic, respectively. The thickness ratio [Moffet *et al.*, 2010b]
 78 can then be calculated by combining equations S3 and S4:

79

$$80 \quad \frac{d_{org}}{d_{in}} = \frac{OD_{320}\mu_{in,278}\rho_{in} - OD_{278}\mu_{in,320}\rho_{in}}{OD_{278}\mu_{org,320}\rho_{org} - OD_{320}\mu_{org,278}\rho_{org}} \quad \text{Equation S5}$$

81

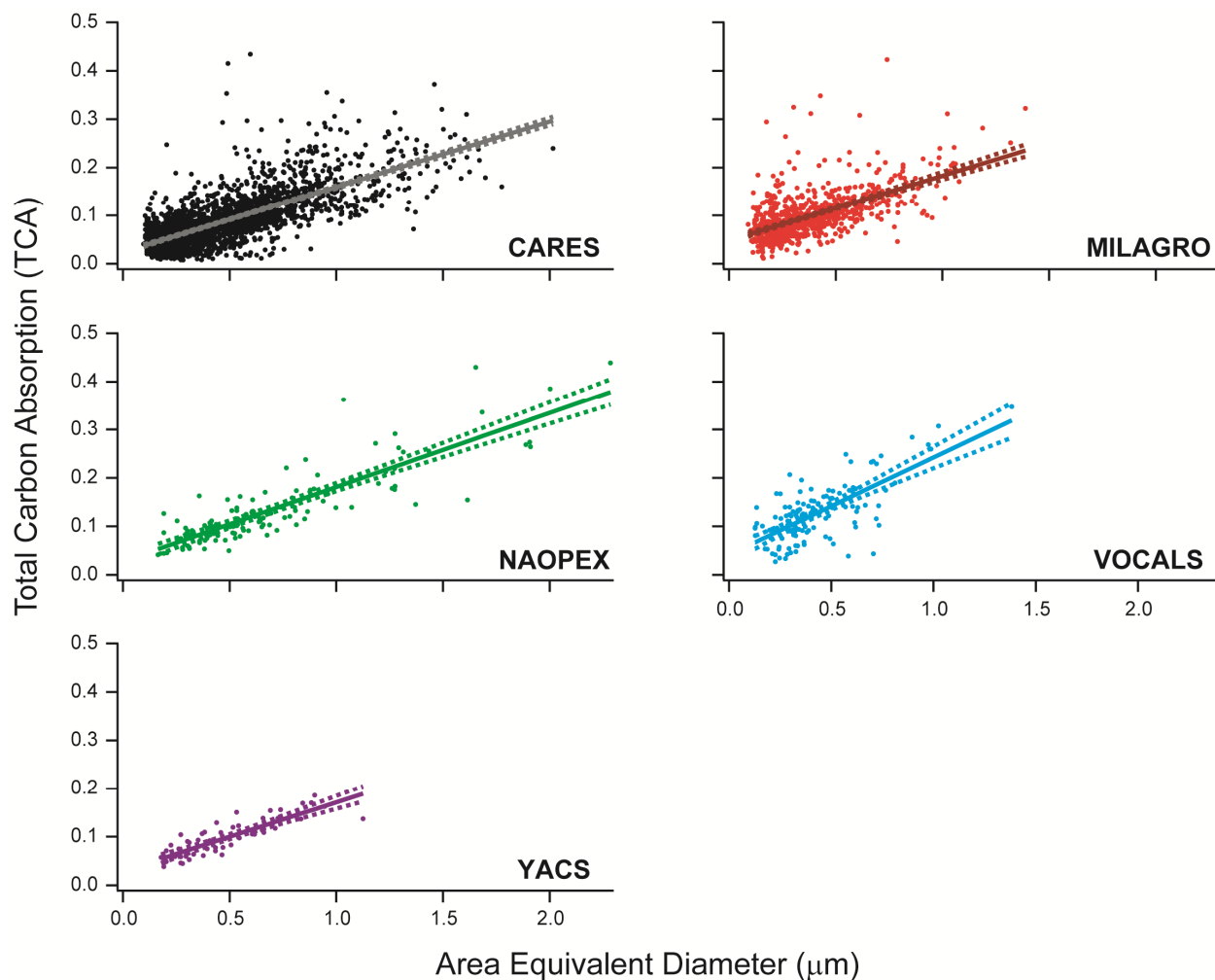
82 To calculate the linear absorption coefficients for the organic terms, the μ_{320} and μ_{278} estimates
 83 from above and a density of 1.3 g/cm³ [Setyan *et al.*, 2012] were used. For the inorganic terms,
 84 three cases were considered. In the first case, the linear absorption coefficients were calculated
 85 for elements with atomic numbers between 6 (carbon) and 26 (Iron) that have been observed in
 86 atmospheric aerosols [Moffet *et al.*, 2010a]. Elements with higher linear absorption coefficients
 87 will absorb more photons and at 278 eV Al, Si, P, S, Cr, Mg, and Fe all have higher linear
 88 absorption coefficients in the range of 7-13 μm^{-1} (Figure S4a). At 320 eV the elements Si, P, S,
 89 Cl, Cr, Mn, and Fe all have coefficients between 5.6-10 μm^{-1} (Figure S4b). Given these ranges,
 90 values of 10 μm^{-1} at 278 eV and 8 μm^{-1} at 320 eV were used. In the second case, the linear

91 absorption coefficients for NaCl were used ($8.1 \mu\text{m}^{-1}$ at 278 eV and $6.3\mu\text{m}^{-1}$ at 320 eV). In the
92 last case, values for ammonium sulfate were used ($3.2 \mu\text{m}^{-1}$ at 278 eV and $2.4 \mu\text{m}^{-1}$ at 320 eV).
93 Using these estimates and the measured OD_{278} and OD_{320} values, the average thickness ratio for
94 each data set was calculated and is shown in Table S4. All of the data sets range from ~10-30%
95 inorganic with higher percentages when all of the inorganic is assumed to be ammonium sulfate
96 as the inorganic. Thus, for these campaigns, approximately 11-30% of the thickness for the
97 organic particles is likely due to the absorption cross section contribution from non-organic
98 molecules or atoms.

99

100 **References**

- 101 Henke, B. L., et al. (1993), X-Ray Interactions - Photoabsorption, Scattering, Transmission And
102 Reflection at $E=50\text{-}30,000$ EV, $Z=1\text{-}92$ (VOL 54, PG 181, 1993). *Atom. Data Nucl. Data*
103 *Tables 55(2): 349-349.*
- 104 Moffet, R. C., et al. (2010a), Microscopic characterization of carbonaceous aerosol particle aging
105 in the outflow from Mexico City, *Atmospheric Chemistry and Physics 10(3): 961-976.*
- 106 Moffet, R. C., et al. (2010b), Automated Chemical Analysis of Internally Mixed Aerosol
107 Particles Using X-ray Spectromicroscopy at the Carbon K-Edge, *Anal Chem 82(19): 7906-*
108 *7914.*
- 109 Setyan, A., et al. (2012), Characterization of submicron particles influenced by mixed biogenic
110 and anthropogenic emissions using high-resolution aerosol mass spectrometry: results from
111 CARES, *Atmospheric Chemistry and Physics 12(17): 8131-8156.*
- 112 Thomson, A., et al. (2009). *Center for X-Ray Optics and Advanced Light Source X-Ray Data*
113 *Booklet.* Lawrence Berkeley National Laboratory, Lawrence Berkeley National Laboratory.



114

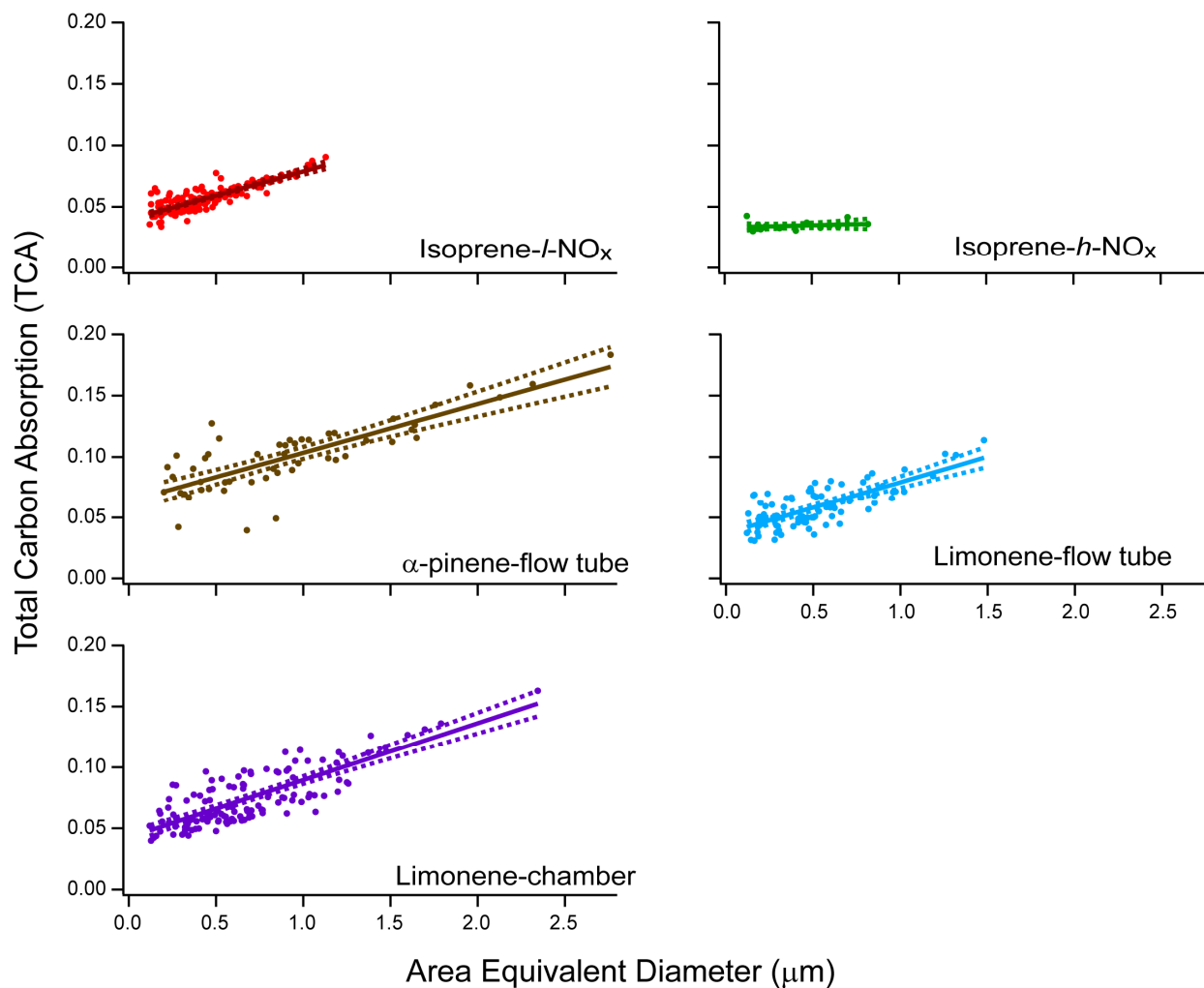
115

116 **Figure S1.** Optical thickness of carbon (total carbon absorption = $OD_{320} - OD_{278}$) as a function of
 117 size of impacted organic particles for each ambient data set. Solid lines are best fit lines for each
 118 data set and dashed lines are $\pm 95\%$ confidence intervals. The thick fitted lines are reproduced in
 119 Figure 2 of the main text, and the slopes, intercepts, and confidence intervals are listed in Table

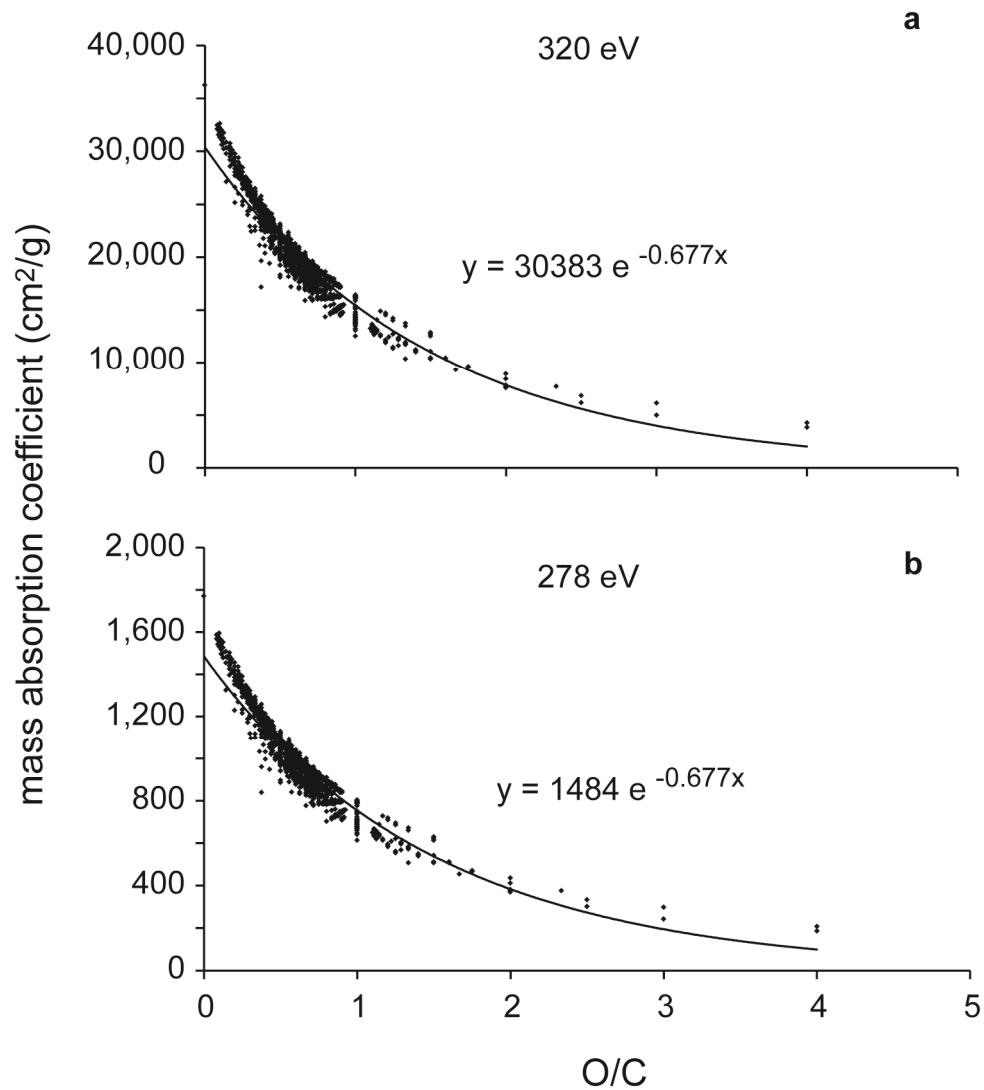
120 1.

121

122



123
 124 **Figure S2.** Optical thickness of carbon (total carbon absorption = $\text{OD}_{320} - \text{OD}_{278}$) as a function of
 125 size of impacted organic particles for each laboratory data set. Solid lines are best fit lines for
 126 each data set; the same lines are reproduced in Figure 2 of the main text. The slopes are listed in
 127 Table 1.
 128
 129



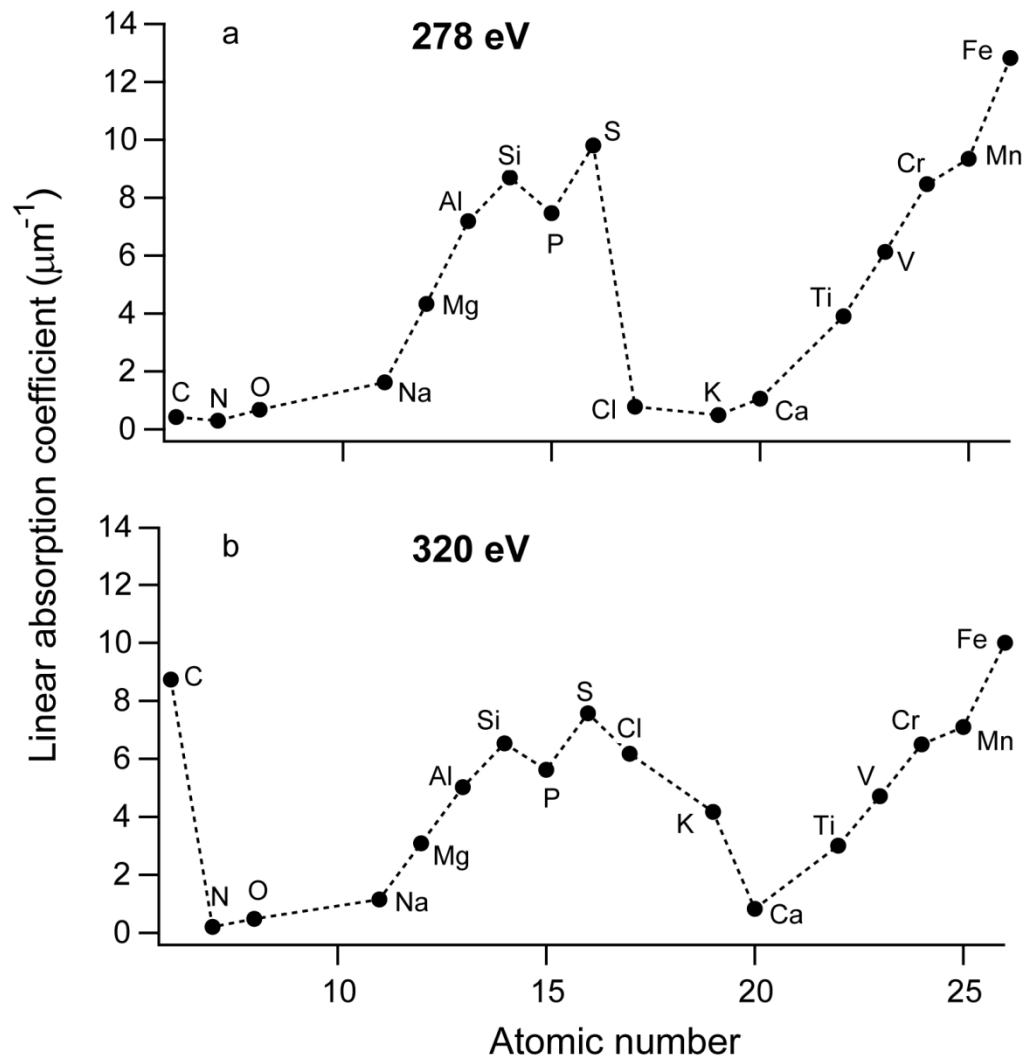
130

131 **Figure S3.** Calculated mass absorption coefficients as a function of O/C at a) 320 eV and b) 278

132 eV for chemical formulas from organic molecules found in atmospheric aerosols.

133

134



135
 136 **Figure S4.** Linear absorption coefficients at (a) 278 eV and (b) 320 eV for elements found in
 137 atmospheric aerosols [Henke *et al.*, 1993].

138
 139
 140
 141
 142
 143

144 **Table S1.** Ambient sample collection information and fitting results for OD₃₂₀ and OD₂₇₈ vs.
 145 area equivalent diameter^a

Campaign	Year	Number of particles	320 eV		278 eV	
			Slope	Intercept	Slope	Intercept
CARES	2010	2428	0.18±0.007	0.041±0.004	0.045±0.002	0.016±0.001
MILAGRO	2006	798	0.19±0.015	0.068±0.006	0.057±0.005	0.019±0.002
NAOPEX	2001	123	0.22±0.022	0.036±0.018	0.069±0.007	0.008±0.006
VOCALS	2008	125	0.30±0.056	0.065±0.027	0.098±0.02	0.023±0.01
YACS	2002	56	0.17±0.028	0.056±0.015	0.027±0.01	0.025±0.006

146 ^aThe ±95% confidence intervals for the slope and intercept are given.

147
 148
 149
 150
 151
 152
 153
 154
 155
 156
 157
 158
 159
 160

161 **Table S2.** Laboratory sample fitting results for OD₃₂₀ and OD₂₈₇ vs. area equivalent diameter^a

Sample	MOUDI stage	Number of particles	320 eV		278 eV	
			Slope	Intercept	Slope	Intercept
Isoprene- <i>l</i> -NO _x	7	137	0.048±0.004	0.054±0.002	0.0083±0.002	0.014±0.001
Isoprene- <i>h</i> -NO _x	7	16	0.018±0.010	0.044±0.004	0.015±0.007	0.011±0.003
α-pinene-flow tube	7	51	0.044±0.009	0.079±0.010	0.0042±0.001	0.015±0.001
Limonene-flow tube	7	87	0.045±0.009	0.051±0.005	0.0027±0.002	0.014±0.001
Limonene-chamber	8	122	0.052±0.007	0.057±0.006	0.0049±0.002	0.015±0.001

162 ^aThe ±95% confidence intervals for the slope and intercept are given. *l*-NO_x and *h*-NO_x refer to
 163 low-NO_x and high-NO_x oxidation by OH; ozone is used as the oxidant for the remaining
 164 samples.

165
 166
 167
 168
 169
 170
 171
 172
 173
 174
 175
 176
 177

178 **Table S3.** Summary of experimental conditions for the chamber experiments^a

Sample	[HC]	Oxidant	[NO]	[NO _y]	[O ₃]	T	Concentration	Average
	ppm	precursor	ppb	ppb	ppb	(°C)	n (μg/m ³)	Size (nm)
Isoprene- <i>l</i> -NO _x	1.0	H ₂ O ₂	<1	5	3	25	40.8	326
Isoprene- <i>h</i> -NO _x	1.1	H ₂ O ₂	430	530	4	24	192	174
Limonene ^b	0.30	Ozone	<1	6	590	24	1251	177

179 ^aThe [HC] are the initial mixing ratios after injection of the liquid precursor, the remaining
 180 values were measured at the start of the sample collection.

181 ^bThe Limonene chamber experiment was done in the dark.

182

183

184

185

186

187

188

189

190

191

192

193

194

195

196

197

198 **Table S4.** Average organic to inorganic thickness ratios for each campaign

Campaign	d_{org}/d_{in} (% of thickness that is inorganic)		
	In = S, metals, etc.	In=NaCl	In=(NH ₄) ₂ SO ₄
CARES	12 (10%)	9.4 (12%)	3.2 (28%)
MILAGRO	9.7 (9%)	7.9 (11%)	2.7 (26%)
NAOPEX	12 (9%)	9.6 (10%)	3.2 (25%)
VOCALS	9.5 (11%)	7.7 (13%)	2.6 (30%)
YACS	12 (9%)	10 (10%)	3.4 (25%)

199

200

201

202

203

204

205

206

207

208

209

210

211

212

213